NAL PROPOSAL No. 16

Correspondent: W. A. Wenzel
Experimental Physics
Lawrence Radiation Lab
Berkeley, Calif. 94720

FTS/Commercial 415-843-5501

P-P ELASTIC AND INELASTIC SCATTERING AT SMALL MOMENTUM TRANSFER

A. R. Clark, T. Elioff, A. C. Entis, R. C. Field,
D. Keefe, L. T. Kerth, R. C. P. Sah, W. A. Wenzel,
Plus Graduate Students
Lawrence Radiation Laboratory

June 10, 1970

D R A F T

Bev-1076

June 16, 1970

NAL PROPOSAL

P-P Elastic and Inelastic Scattering at Small Momentum Transfer

Correspondent: W. A. Wenzel LRL, Berkeley

Names of Experimenters:

A. R. Clark,	LRL	D. Keefe,	LRL	
T. Elioff,	LRL	L. T. Kerth,	LRL	
A. C. Entis,	LRL	R. C. F. Sah,	LRL	Plus Graduate Students
R. C. Field,	LRL	W. A. Wenzel,	LRL	

ABSTRACT

We propose to measure pp elastic and inelastic scattering cross-sections for momentum transfers $|t| \sim 0.001$ to $|t| \sim 0.1$. The experiment would use a magnetic spectrometer with a calibrated gas target in the main ring circulating beam to obtain absolute cross-sections. The apparatus would be suitable for incident protons in the range 10-500 GeV/c, and will be usable for the study of proton scattering from other nuclei. The apparatus would take data over the full energy range during the acceleration cycle.

II. Physics Justification

In the high energy region the small angle scattering of strongly interacting particles is capable of explanation in terms of a diffraction effect from an absorbing volume which is readily identifiable with the classical nucleon or nuclear size as determined by other means. Although it was known by 1957 that this effective nucleon size at high energy increases with increasing energy,[1] no particular significance was attached to it until the development of the Regge Pole model,[2] in which the changing t dependence of the small angle elastic scattering cross-section was identified with the slope of the Pomeron trajectory. Measurements of the pp cross-section at higher energies have generally indicated that the shrinking diffraction pattern persists, but other elastic scattering interactions have not shown this effect;[3] hence it is obvious that the single trajectory Regge Pole model is not sufficient below 30 GeV. It has been shown, however, that the inclusion of trajectories other than the Pomeron will generally provide a satisfactory description of the data.[4]

If Pomeron exchange dominates elastic scattering processes and the trajectory is linear, the nuclear scattering amplitude will be of the form

$$fn = f(t)e^{b\ t\ \ln\ s}$$

At the highest energies yet measured the Dubna group[5] has found a good fit to their data using

$$fn = f_o e^{\frac{b_o t + b_1 t \ln s}{2}}$$

where f_o is the optical amplitude, s is measured in GeV,^{2} $b_o = 6.8 \pm 0.3$ $(GeV/c)^{-2}$ and $b_1 = 0.47 \pm .09$ $(GeV/c)^{-2}$

The relative importance of the Pomeron, as the highest lying Regge

trajectory is expected to increase at higher energies; but this is only one justification for elastic scattering measurements at NAL. It has been argued that the behavior of the differential cross-section is fundamental to the features of asymptopia; Bessis[6] has shown that the Froissart bound implies a limit of $(\ln s)^2$ on the rate of increase of the slope parameter. Other interest in the elastic cross-section measurements centers centers around the amount of real part in the cross-section and its effect in the couloumb interference region. Up to 26 GeV there is a considerable amount of real part in the scattering amplitude.[7] Measurement of the real part requires accurate absolute calibration, because the amplitude is generally dominated by the imaginary part of the nuclear amplitude and (at small t) by the coulomb amplitude. A forward nuclear amplitude greater than the imaginary part calculated from ordinary total cross-section measurements will also occur if the singlet and triplet pp total cross-sections differ.

The production of nucleon isobars below 30 GeV proton energy has been observed over a variety of energies and momentum transfers.[8][9][10] At large t the cross-sections compare with those for elastic scattering. At intermediate t the cross-sections for producing some of the known states are 1-10% of the elastic cross-section and relatively independent of energy. The t dependences of the cross-sections for production of the various isobars are quite different for $|t| < 1\ \mathrm{GeV}/c^2$ [9], presumably reflecting different exchange mechanisms.

At higher energies and low $|t|$ quite different behavior can be expected between e.g.

$$p_1 + p_2 \rightarrow p_3 + N^*(1238) \text{ and}$$

$$p_1 + p_2 \rightarrow p_3 + N^*(1430)$$

because the latter process can proceed by Pomeron exchange

(diffraction dissociation) while the former should be dominated by pion exchange, for which the effect will decrease below $-t = m_\pi^2 \approx 0.02$ GeV/c^2. Generally we expect that production at very low t will be relatively important for isobars in the series $1/2^+$, $3/2^-$, $5/2^+$, etc. Possible use of symmetric nuclei (He, C, etc.) as targets provides an interesting possibility for the general study of the diffraction dissociation of the proton.

III. Experimental Arrangement

A. Kinematics

A major problem in the use of a single arm spectrometer is in separating elastic from inelastic scattering. For the process

$$P_1 + P_2 \rightarrow P_3 + P_4$$

detection of P_3 leads to the following expression for missing mass M_4.

$$M_4^2 = M_1^2 + M_2^2 + M_3^2 + 2M_2E_1 - 2E_3(M_2 + E_1) + 2P_1P_3\cos\theta_3 \qquad (1)$$

In the general case where $M_1 = M_2 = M_3 = M$ are protons we may write for the mass resolution near $M_4 = M$

$$\left(\frac{\partial M}{\partial E_1}\right)_{\theta_3, P_3} = \frac{E_3 - M}{E_1 - M} \quad ; \left(\frac{\partial M}{\partial \theta_3}\right)_{E_1, P_3} = -\frac{P_1 P_3 \sin\theta_3}{M} \qquad (2)$$

$$\left(\frac{\partial M}{\partial P_3}\right)_{E_1, \theta_3} = -\frac{(E_1 + M)P_3}{(E_3 + M)E_3}$$

The resolution must be adequate separately with respect to each of the three variables E_1, P_3, θ_3. For the large angle recoils it is obvious that the dependence on E_1 is extremely small. For elastic scattering this will permit us to take data for the whole range of P_1 using the same set-up. Resolution in both θ_3 and P_3 is limited by instrumental considerations. θ_3 is also limited by coulomb scattering and P_3 by range straggling. The effect of the latter has approximately the same momentum dependence as does coulomb scattering, which is far more important for the thin targets considered here. Figure 1 shows the worst resolution in each quantity that can be tolerated at 200 GeV for a 0.1 GeV mass resolution. Errors add incoherently. The problems become more difficult with P_1 linearly for $\frac{\Delta P_3}{P_3}$ and $\delta\theta_3$ and quadratically for the thickness x relative to radiation length x_o. To get down to $|t| = .001$ at 200 GeV therefore, we will need to find $\frac{x}{x_o} \lesssim 10^{-6}$, and to get up to $|t| = 0.1$ we need $\delta\theta_3 \lesssim 1.5 \cdot 10^{-3}$ and $\frac{\Delta P_3}{P_3} \lesssim 10^{-2}$.

B. Spectrometer

Two spectrometer designs are under consideration. One is the orthogonal dispersion spectrometer[11] developed for a series of Bevatron experiments during 1963-64.[10][12][13] (Figure 2) Data taken with a gaseous hydrogen target is shown in Figure 3. In this case the gas was at one atmosphere pressure and secondaries from a single pass of the external proton beam at $\approx 10^{11}$ protons per burst were detected. At NAL energies such a target would not be useful primarily because of the loss of resolution associated with scattering in the gas and the 10^{-3} in mylar window.

The orthogonal dispersion spectrometer has several advantages in this kind of experiment

(1) It can look at an extended source without loss of resolution in θ_3. Hence the data rate can be relatively high.

(2) The detector can be located at a considerable distance from the beam. Together with magnetic analysis this permits detailed shielding to be done.

(3) The electronics associated with the use of the spectrometer is relativily simple because the detector is located in a single image plane. This is especially appropriate here where the particles haven't enough range to traverse a multiple detector system.

The spectrometer layout in Figure 4(a) is designed to provide a large horizontal focal length (250-in), a reasonably large dispersion at the image plane (D ≈ 50-in) and a demagnified image of the target (M ≈ 0.2) The latter feature is desirable because at injection the target is about the size of the useful accelerator aperture (≈ 2-in) vertically. Presumably the beam size decreases with energy as $[P]^{-1/2}$ because of adiabatic damping of the betatron oscillations.

A variation of the spectrometer design, also under consideration, is shown in Figure 4(b). This uses a lens system as in 4(a) to accept a large target size and provide a long horizontal focal length for angular resolution. Instead of the strong dispersing magnet, however, solid state counters would be used to define the momentum width through pulse height analysis. The latter have been used by the Dubna group at Serpuhkov.[5] Resolutions $\frac{\Delta T_3}{T_3} = 2\,\frac{\Delta P_3}{P_3} \approx (1\text{-}2)\ 10^{-3}$ are possible in this energy range,[14] although it may be difficult to make counters thick enough for $|t| = 0.1$ (≈ 3 g cm^{-2}). Also large area solid state counters are hard to make. Nevertheless we consider as a possibility their use with the spectrometer.

In either case two lenses only are needed to provide a double focus in the image plane. With three lenses, as indicated, a trade can be made between resolution and rate. This is especially relevant to the cross-section measurements of nucleon isobars, where at small P_1 and t the mass scale should be compressed (or the horizontal focal length decreased) to increase the signal to noise ratio in the counters, and at large P_1 and t, as has been noted, maximum expansion of the mass scale is needed for resolution.

A small deflecting magnet is needed (Figure 4) to correct for the variation in proton production angles with P_3 (and M_4). For the range of interest this deflection is small $\int B\, d\ell \sim 10^4$ gauss-in so that the magnet is small and easily shielded from the accelerator.

An important feature of the spectrometer in the configuration of Figure 4(a) or (b) is that the yield, which is proportional to the spectrometer constant $\frac{\Delta P_3}{P_3}$ and the azimuthal acceptance $\Delta\phi$; depends on only the dispersing magnet (or counter resolution) and not on lens aberrations, provided that the target itself contributes a resolution width smaller than that accepted in the image plane.

C. The Target

A gas target of the type used in the earlier Bevatron experiment is impractical for reasons given previously. Recently the Dubna group has begun use of a hydrogen jet to provide a low density internal target.[15] The disadvantage of this method is that absolute calibration is difficult; it has been suggested that the pure coulomb/amplitude scattering at very low t be used for this purpose.[15]

To avoid the difficulties associated with uncertain gas concentrations we propose to use for a target a gas volume with a well defined and measurable pressure and density. This is shown in Figure 5. In order to provide for accurate

measurements of the gas concentration a stagnant target volume is provided between two input manifolds. The hydrogen is exhausted along the main beam line through differentially pumped apertures restricted to slightly more than the beam size.

L. Teng estimates[16] that at injection an average pressure of 10^{-6} mm of hydrogen is tolerable and that at the higher energies (> 30 GeV) five times this amount could be used. This corresponds to local gas thicknesses of 6.28 micron meters and 31.4 micron meters respectively. Hence it is possible to consider two modes of operation, gated and continuous, with different data rates available. For the gated case it would be essential for normalization that equilibrium is reached before taking data. Because the velocity of hydrogen gas is $\sim 10^5$ cm/sec at room temperature and the characteristic length of the target is 30 cm, we would expect to reach equilibrium in a few milliseconds. The higher pressure, even without accurate calibration, could be useful in the isobar measurements.

In what follows, however, we consider the continuous flow case with a 10 micron pressure gas target of length L_t = 30 cm, and we adjust the flow rate to give a 6.28 micron-meter total path length. The accelerator beam tube is assumed to be 2-in x 5-in in cross-section. The molecular mean free path is 0.9 cm at 10 microns.[17] Hence we are (barely) in the viscous flow region, for which the Poiseuille equation[17] gives

$$Q = \frac{\pi a^4}{16\eta} \frac{dP^2}{d\ell} = \frac{A^2}{16\pi\eta} \frac{dP^2}{d\ell} \tag{3}$$

for the flow rate in micron cm^3 sec^{-1} through a cylinder, where a is the radius (or A the area) and ℓ the length in centimeters, P is in microns and η is the viscosity (9.10^{-5} for hydrogen). Loevinger has proposed a formula for rectangular pipes.[17] For air at 25° C this gives

$$Q = 0.13\ Y\ A^2 \frac{dP^2}{d\ell} \tag{4}$$

where Y is a factor less than or equal to one which depends on the aspect ratio. (For the assumed pipe Y=0.71). Putting back in the viscosity of air (18.10^{-5}) we obtain a general formula

$$Q = .0234 \frac{Y\ A^2}{\eta} \frac{dP^2}{d\ell}\ cm^3\ sec^{-1} \tag{5}$$

in good agreement with (3)

In our case therefore

$$QL_e = 7.0.10^4 \text{ micron liter cm } sec^{-1} \tag{6}$$

where L_e is the length of each exhaust pipe. For the pressure distribution given by (5) the total gas thickness seen by the beam is $P_o(L_t + 4/3\ L_e) = 6.28$ micron meter. For P_o = 10 and L_e = 0.3 we find that L_T = 0.25 m. Substituting in (6) we find on each side Q = 2800 micron liters per sec., which is achievable with standard pumping techniques. With these parameters about half the beam-gas interactions are in the useful target volume.

We have assumed that the spectrometer is directly coupled to the target. It will have a volume of more than a hundred liters and would therefore take a reasonable fraction of a second to fill up if the target is "gated". In this case it would be useful to have a flap valve at the upstream end of the spectrometer to preserve pressure between pulses. This could be operated by a rotary solenoid and would probably be needed anyway in order to let the spectrometer be opened to air at the detector end.

At a pressure of 10 microns of hydrogen it is readily shown that coulomb scattering and range straggling are completely negligible in the worst case. Attenuation of the circulating beam would be of the order of one part in 10^4. This too is probably negligible.

It is desirable that the side and back walls of the target be kept clear of the circulating beam to reduce spurious background. We can set some limits on background from interactions of this type by assuming some beam loss distributed uniformly around the machine. Suppose this is as much as 1%; then because the target covers only about one part in 2.10^4 of the circumference we expect a primary interaction rate of order 10^{-6}, two orders of magnitude less than that from the gas; secondary processes are harder to estimate. To reduce the background further, shielding around the beam pipe could be added upstream of the target to cover those surface of the target volume that can be seen by the spectrometer.

Measurement of the gas pressure is essential to the absolute calibration. We propose to use a frequently calibrated ion gauge, from which the electrical signal would be monitored continuously.

A mumetal shield around the target volume will eliminate any stray field at the radius of the circulating beam.

D. The Detector

The detector (Figure 6) includes primarily a series of counters in the image plane

of the spectrometer. For the orthogonal dispersion spectrometer these consist of a scintillator hodoscope and other scintillation counters which can be used in coincidence when protons of sufficient range are involved. The hodoscope is rotated in the plane perpendicular to the axis of the spectrometer through a chromatic rotation angle[11] which places all secondaries associated with a given missing mass along the line of the hodoscope. In this way a large momentum bite, limited only by chromatic aberration, can be accepted without loss of resolution. It appears that for $\delta\theta \approx 10^{-3}$ the counters should be $\lesssim 0.25$-in wide. The counters should be thin so that edge effects are small. The more energetic protons will penetrate the hodoscope counters, so that coincidences may be used above, say, 150 MeV/c (for 1/16-in scintillators) and anticoincidence may be used below this momentum to reject background. An adjustable collimator is also included to select the momentum width of the spectrometer.

Use of solid state counters would be simpler on the one hand because the detector would not need to be rotated. The electronics would be somewhat more complicated, however, because pulse height analysis would be needed for each of the hodoscope counters.

E. Cross-Section Measurement

The counting rate is given by the following expression

$$N = N_b N_t \frac{d\sigma}{dt}\, dt\, \frac{d\phi}{2\pi} = 2N_b N_t \frac{d\sigma}{dt}|t|\frac{dp}{p}\frac{d\phi}{2\pi} \qquad (7)$$

At 10 microns (continuous flow case) with a 20 cm target length we find

$N_t = 1.43.10^{16}$ atoms per square cm.

For a 1 km radius accelerator at 10^{13} protons per burst

$N_b = 4.8.10^{17}$ protons per second.

For an average $|t| = 0.01$ we have

$$\frac{d\phi}{2\pi} \approx .02\ ,\quad \frac{dp}{p} \approx .05\ ;\quad \frac{d\sigma}{dt} \approx 10^{-25}$$

for this (7) gives

$n \approx 13800$ counts per second (continuous flow case)

Note that $d\phi$, dp and the target length are all determined by

precision collimators. Measurement of the circulating beam intensity should be based on the use of electrostatic pickup plates, requiring a measurement of capacitance, length, and voltage together with some slight knowledge of the azimuthal bunch structure. A counter telescope provides a secondary monitor. It should be calibrated from the circulating beam monitor. It can be located (Figure 4) so that it automatically compensates for errors in $\Delta\phi$ caused by any in-out displacement of the beam in the target volume.

F, Data Collection

We propose to use a small computer (PDP-5 or larger) to accumulate data during the acceleration cycle. The arrangement would be similar to that used by Ankenbrandt et al.[12] Each hodoscope channel would feed a scaler. At the end of a preselected energy interval the data-taking would stop and each channel would be fed into the computer $\approx$ 1 word per channel including that for the monitor. This could involve up to 30 channels so the total read-in time would be a small part of the accelerating cycle. Note that the data rate for elastic scattering is expected to be uniform in time but the physics probably demands that the lengths of the energy bins be equally spaced on a log scale. This is especially true when isobar measurements are made. Equation (2) shows that the mass scale varies logarithmically with P_1; for the largest value of E_3-M (50 MeV) a twenty percent bin width produces a full width of 10 MeV in the smearing of the mass scale within a given bin. In this way 20 energy bins, for example, could be established between 10 and 500 GeV. Information on magnet currents, collimator settings and pressure would be entered at the beginning and end of each accelerator pulse.

An alternative (necessary if solid-state counters are used) is to read each event directly into the computer. This had the advantage of needing less hardware for buffering and that it permits later arbitrary binning of the data, but its disadvantage ---->

is that it requires careful attention to the monitor to effect normalization, that it requires the explicit entry of time (or energy) for each event and that the procedure generally requires more read-in time for high data rates.

Use of the computer would include the provision of various diagnostic displays presented between accelerator pulses. The data would be read onto tape for analysis on a larger computer.

G. Running Time

This is hard to estimate because it will depend on the accelerator intensity. For the elastic scattering at full beam the rates are easily adequate so that statistics will not be the limit. Even at 10^{11} protons per burst the running time will be short. With 200 counts per burst spread over twenty channels this is 10 per channel per burst average or 10^5 counts per day per channel. Hence with ten settings int, the experiment can be done in one day with one percent statistics. Allowing for changeover time this should be multiplied by about ten. We estimate

Tuneup	200 hours
P-P elastic	200 hours
P-P inelastic	200 hours

Requests for the study of other target materials should await demonstration that the apparatus works.

IV. Apparatus

In view of the fact that there is no internal target area at NAL we consider it important to establish that the proposed experiment is feasible. The location around the ring is not too critical except that several feet tranverse to the beam is needed. The main tunnel may

be too small in width. The spectrometer components shown in Figure 4 are based on existing Bevatron magnets. They would be running at very low field (≤ 400 g/in) in this application. Hence with care in the design of new elements the spectrometer could be compressed in length. As has been stated the extra length is an advantage (if room can be found) because it facilitates shielding.

A long straight section is not needed. About 4 ft. clear along the beam line is enough, provided that a few more meters on either side are available for additional differential pumping to isolate the hydrogen target completely from the sensitive parts of the accelerator. It should not be located where the angular divergence of the beam is greater than 10^{-3}.

The location should provide for easy access and modest cable runs. About 30 high voltage - signal (combined) cables are needed, along with a dozen control cables plus magnet cables. The collimators and magnet currents should be controlled remotely to minimize interference with accelerator operation. In operation the experiment as proposed is compatible with essentially all other use of the machine.

For the preparation of apparatus we propose the following:

A. Detector. This should be built and tested at LRL including hodoscope counters and others, counter monitor, and electronic logic. Short cables could come from LRL. Long runs should perhaps become part of the NAL facility

B. Computer. We assume a standard computer is available. If it does not exist at NAL we will attempt to borrow it from the LRL or another counting pool. In any case we would hope to put together the interface and do testing with a similar computer at LRL. It would be desirable to have similar computers in both laboratories to avoid problems associated with transportation.

C. Spectrometer. The collimators, vacuum system, and magnets used will depend on precise details of location. If it is decided that NAL wants magnets of the type needed, we would propose to use these. Otherwise we would attempt to borrow magnets from the Bevatron or another accelerator. In either case we would assist in the testing and design of new pole tips, shims, etc. The small front dispersing magnet will not be expensive, but it should probably be tailored to this problem specifically. We propose to design the spectrometer vacuum system as well as the collimators, even if NAL magnets are used.

D. Target. We assume that NAL will want to participate closely in the design and construction of this system, if only to defend the accelerator.

E. Schedule. Depending on the availability of the accelerator and magnets, and on NAL's willingness to commission an internal experiment, we believe we can be ready by July 1971.

F. Manpower. Although we believe that our LRL group is scientifically and technically strong enough to carry out the experiment, we would welcome working collaborators particularly from NAL.

References

1. B. Cork, W. A. Wenzel, and C. W. Causey, Phys. Rev. 107, 859 (1957).
2. G. F. Chew and S. C. Frautschi, Phys. Rev. Letters 7, 394 (1961).
3. See for example S. J. Lindenbaum, International Conference on Nucleon Structure, Stanford (1963).
4. R. J. N. Phillips and W. Rarita, Phys. Rev. Letters 14, 502 (1965).
5. G. G. Beznogikh, et al., Phys. Lett. 30B, 274 (1969).
6. J. D. Bessis, Nuovo Cimento 45A, 974 (1966).
7. H. Lohrman, et al., Phys. Letters 13, 78 (1964);
   L. Kirillova, et al., Phys. Lett. 13, 93 (1964);
   A. E. Taylor, et al., Phys. Lett. 14, 54 (1965);
   K. J. Foley, et al., Phys. Rev. Lett. 14, 74 (1965);
   G. Bellettini, et al., Phys. Lett. 14, 164 (1965).
8. G. Cocconi, et al., Phys. Rev. Letters 7, 450 (1961);
   G. B. Chadwick, et al., Phys. Rev. 128, 1823 (1962);
   G. Cocconi, et al., Phys. Letters 8, 134 (1964);
   G. Bellettini, et al., Phys. Letters 18, 167 (1965);
   I. M. Blair, et al., Phys. Rev. Letters 17, 789 (1966).
9. E. W. Anderson, et al., Phys. Rev. Letters 16, 855 (1966).
10. C. M. Ankenbrandt, et al., Nuovo Cimento (10) 35, 1052 (1965). (UCRL-11423.)
11. C. M. Ankenbrandt, et al., IEEE Transactions on Nuclear Science NS-12, 4, 113 (1965). (UCRL-11995).
12. C. M. Ankenbrandt, et al., Phys. Rev. 170, 1223 (1968). (UCRL-17763) also (UCRL-17257, Thesis).
13. A. R. Clyde, et al., International Conference on High Energy Physics, Dubna, 1964. UCRL-11441. Also UCRL-16275, Thesis.

References (continued)

14. F. Goulding et al., Semiconductor Nuclear Particle Detectors and Circuits. National Academy of Science No. 1593, 744 (1969). UCRL-17556.

15. V. A. Nikitin. Private Communication.

16. L. Teng. Private Communication.

17. S. Dushman and J. M. Lafferty, Scientific Foundations of Vacuum Technique, John Wiley and Sons, Inc., New York, London, Second Edition, p. 82-87.

Figure Captions

Fig. 1 Maximum tolerable resolution width for a missing mass error of 0.1 GeV at 200 GeV/c.

Fig. 2 Orthogonal Dispersion Spectrometers used in the experiments of References 10, 11, and 13. The design of the low momentum channel is similar to the one proposed here.

Fig. 3. Data from Reference 13.

Fig. 4 Proposed alternative spectrometers:

(a) Orthogonal Dispersion Spectrometer

(b) Focusing Spectrometer with Solid State Counters

Fig. 5 Continuous Flow Hydrogen Gas Target.

Fig. 6 Detector in Image Plane of Orthogonal Dispersion Spectrometer δ is the chromatic rotation angle defined in Ref. 11.

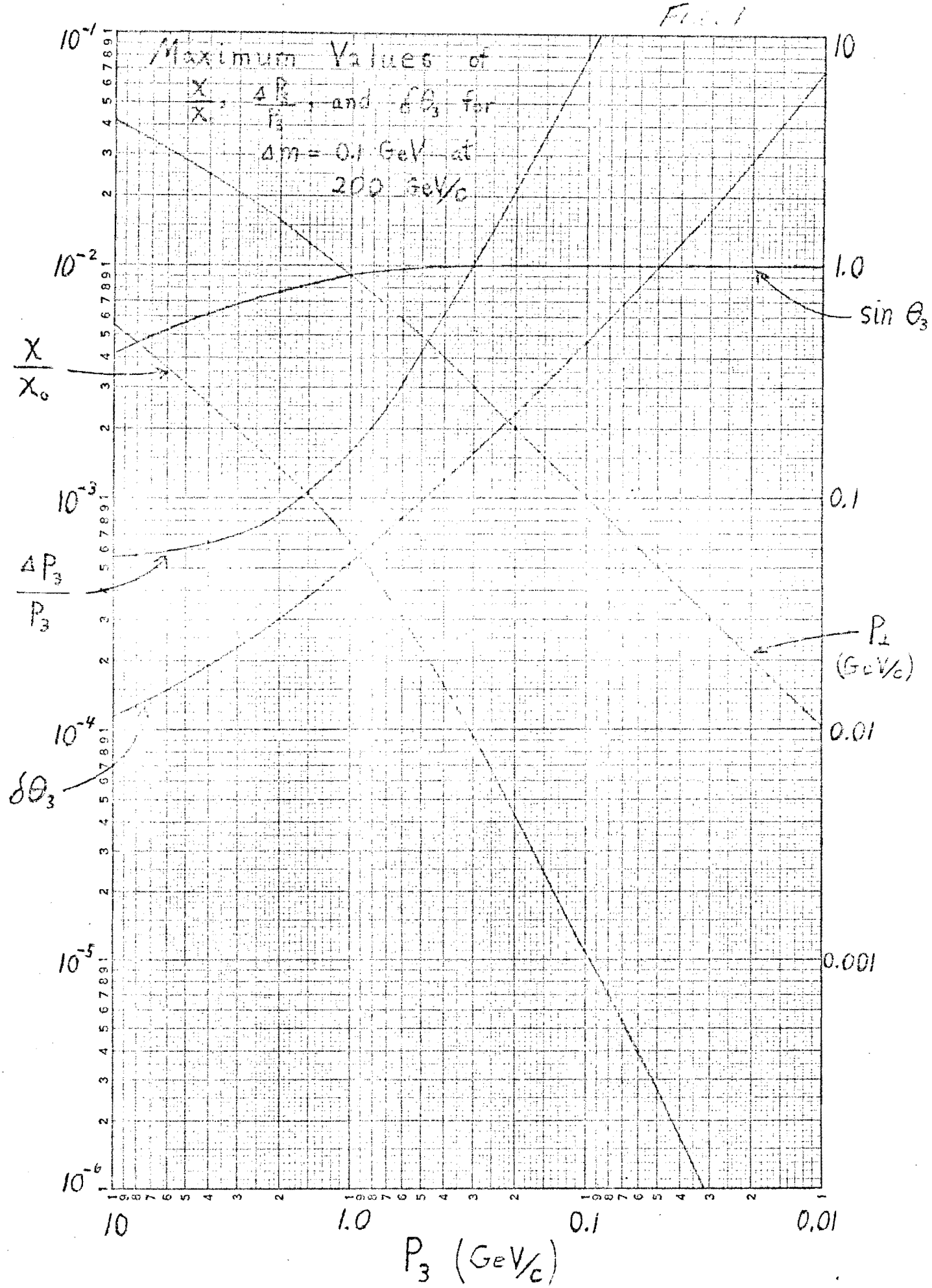

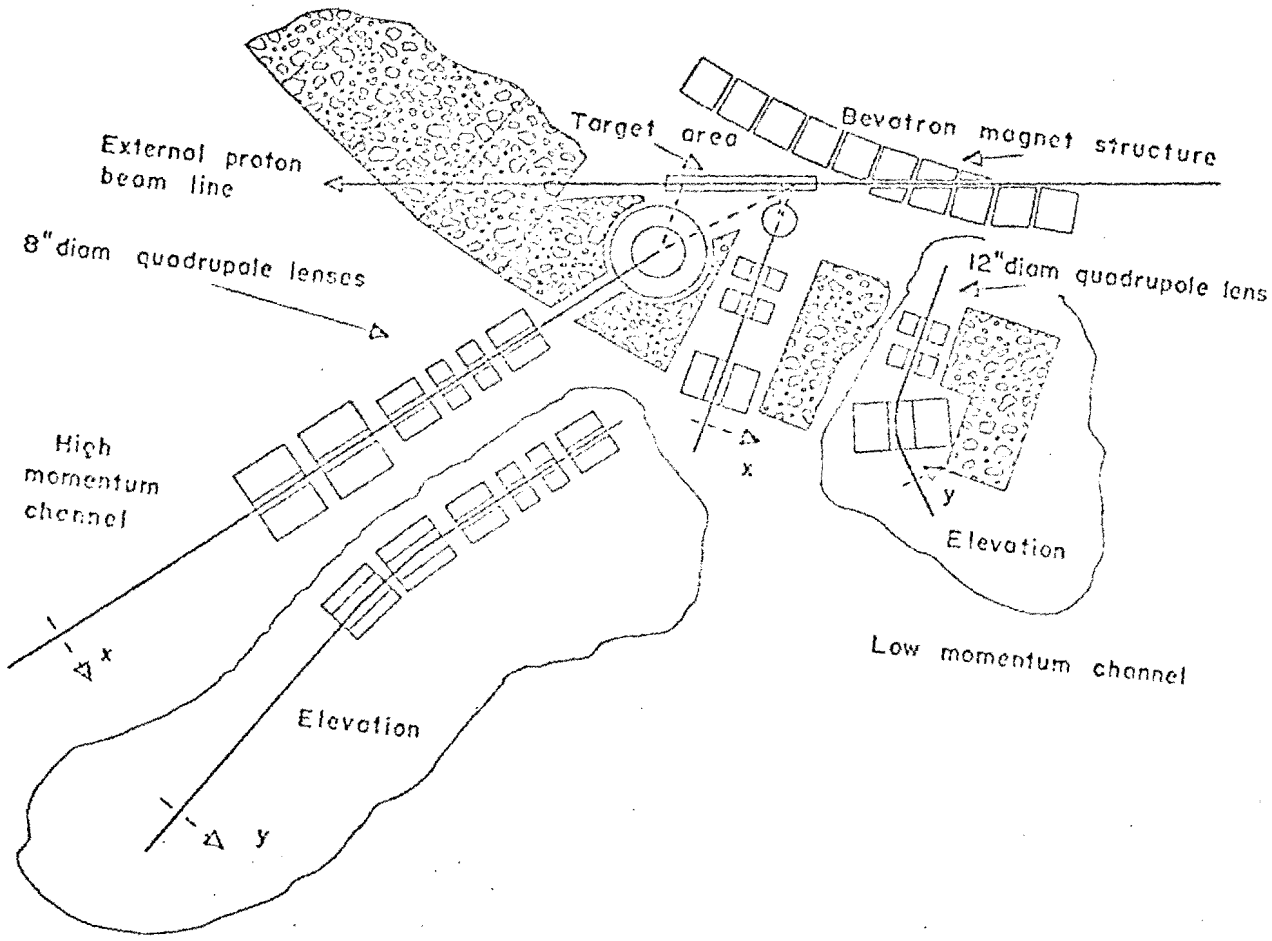
Target area
Bevatron magnet structure
External proton beam line
8" diam quadrupole lenses
12" diam quadrupole lens
High momentum channel
x
y
Elevation
Elevation
x
y
Low momentum channel
MUB-5978

Fig. 2

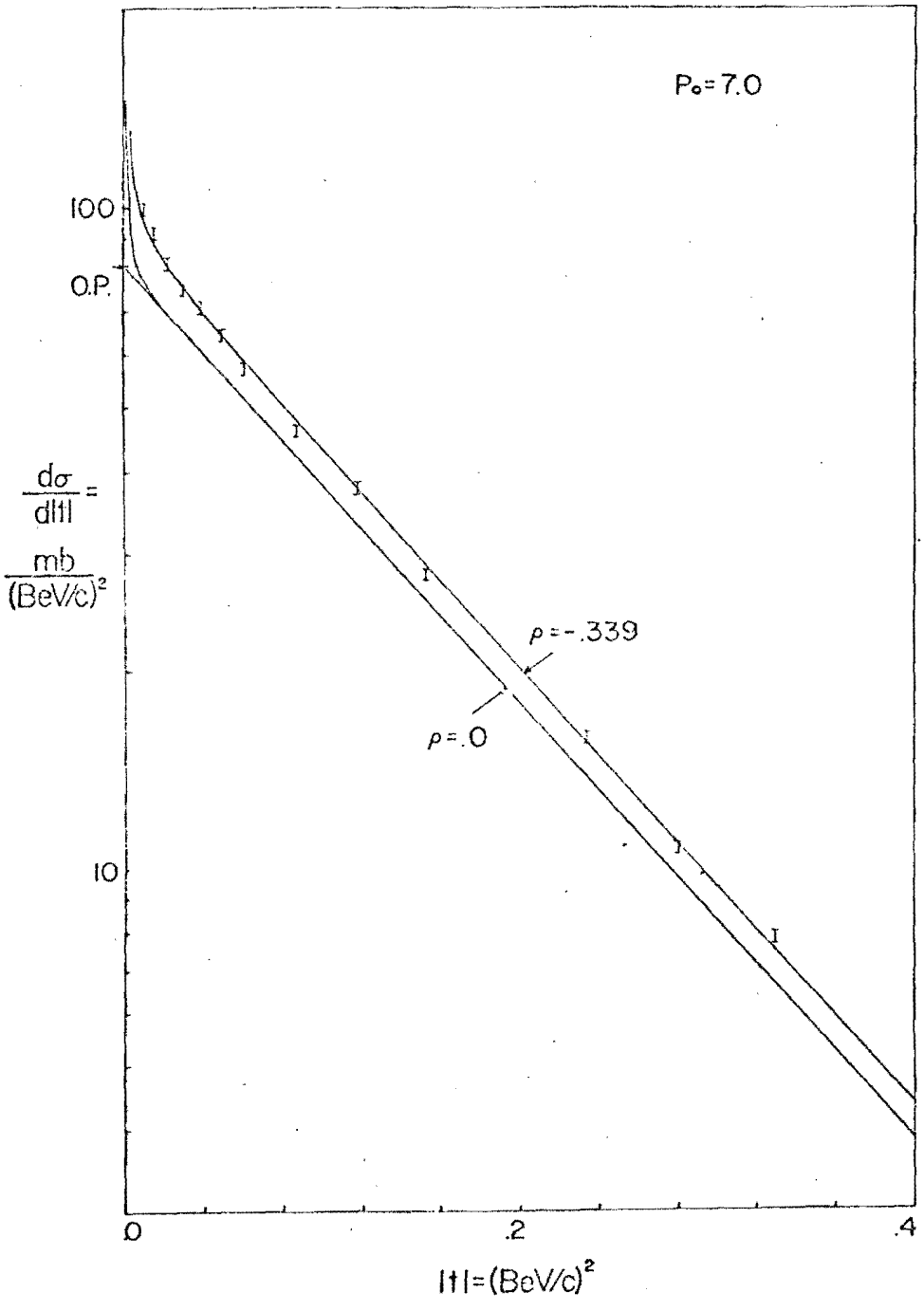

MU-36806

The forward scattering data taken with the hydrogen gas target at incident momentum P_o = 7.0 BeV/c. The upper curve is the theoretical fit to the data points for ρ = −.339. The lower curve is shown for comparison with ρ = 0.

Fig. 9

Shielding

FIGURE 4

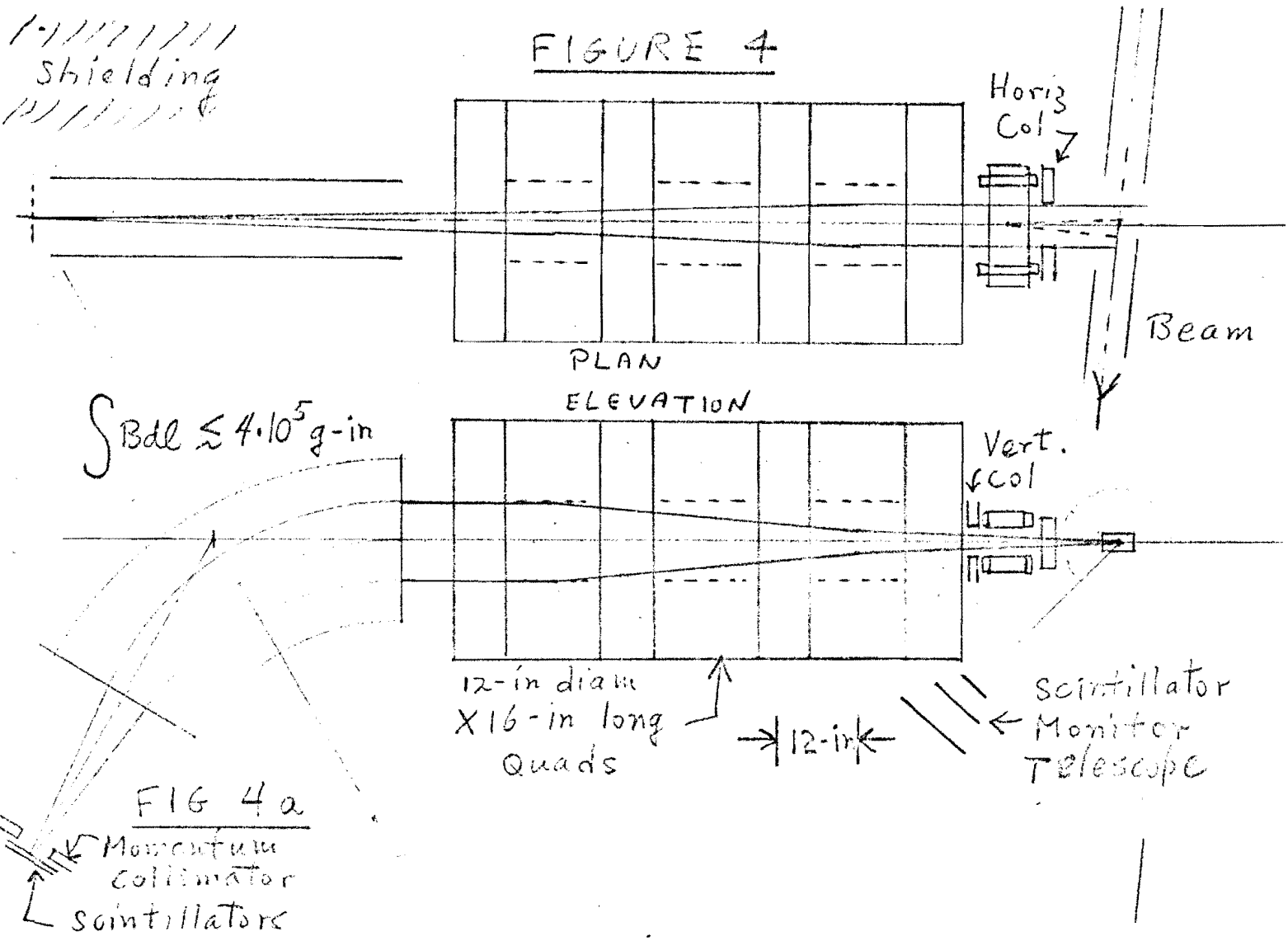

FIG 4a

FIG 4b

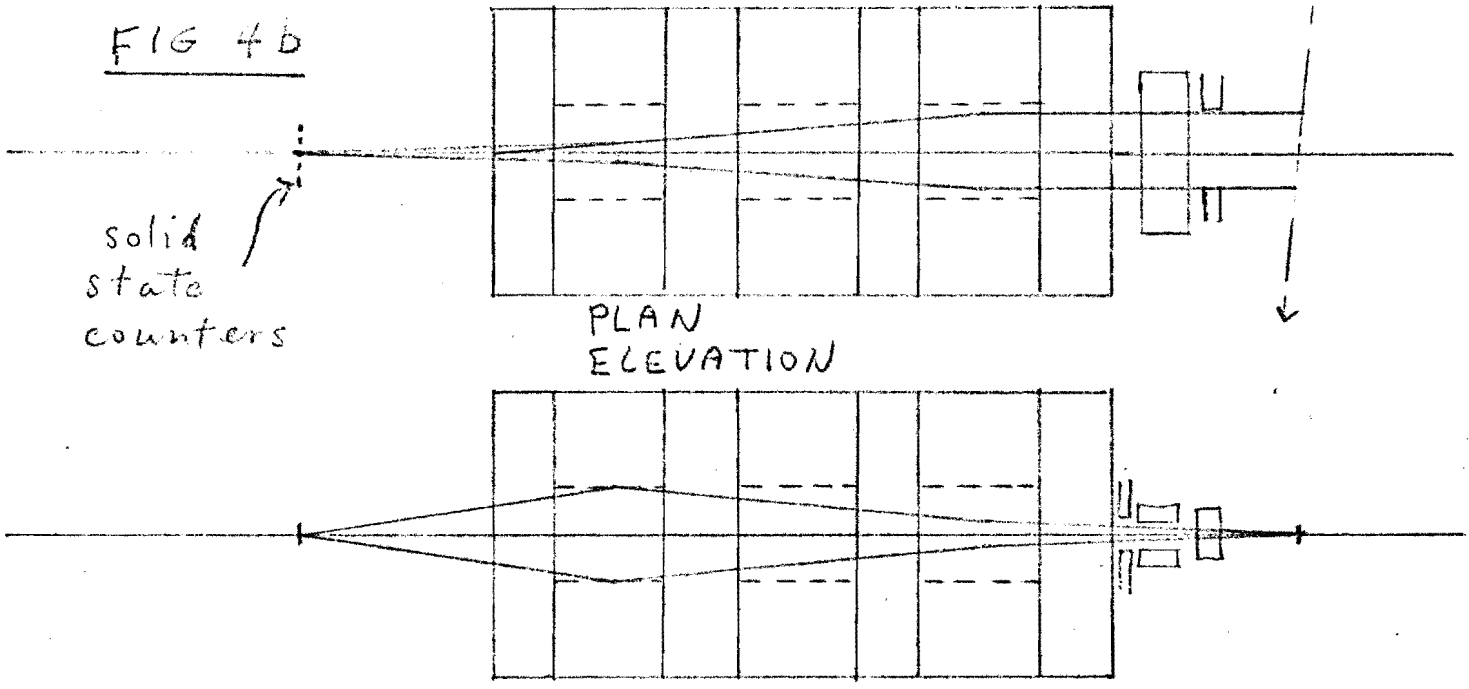

FIGURE 5

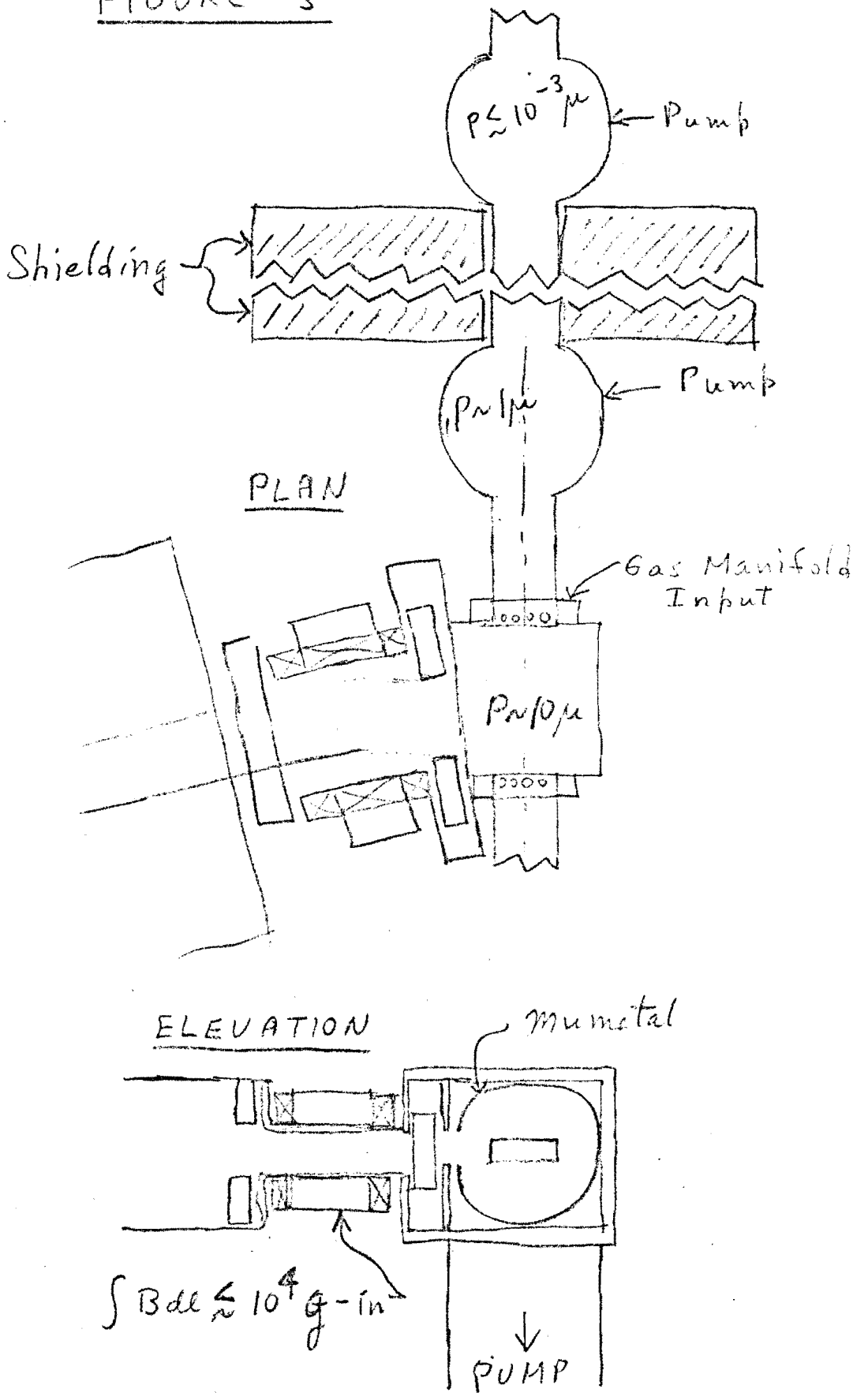
$P \lesssim 10^{-3}\,\mu$
Pump
Shielding
$P \sim 1\,\mu$
Pump
PLAN
Gas Manifold Input
$P \sim 10\,\mu$
ELEVATION
Mumetal
$\int B\,dl \lesssim 10^{4}$ g-in
PUMP

FIGURE 6

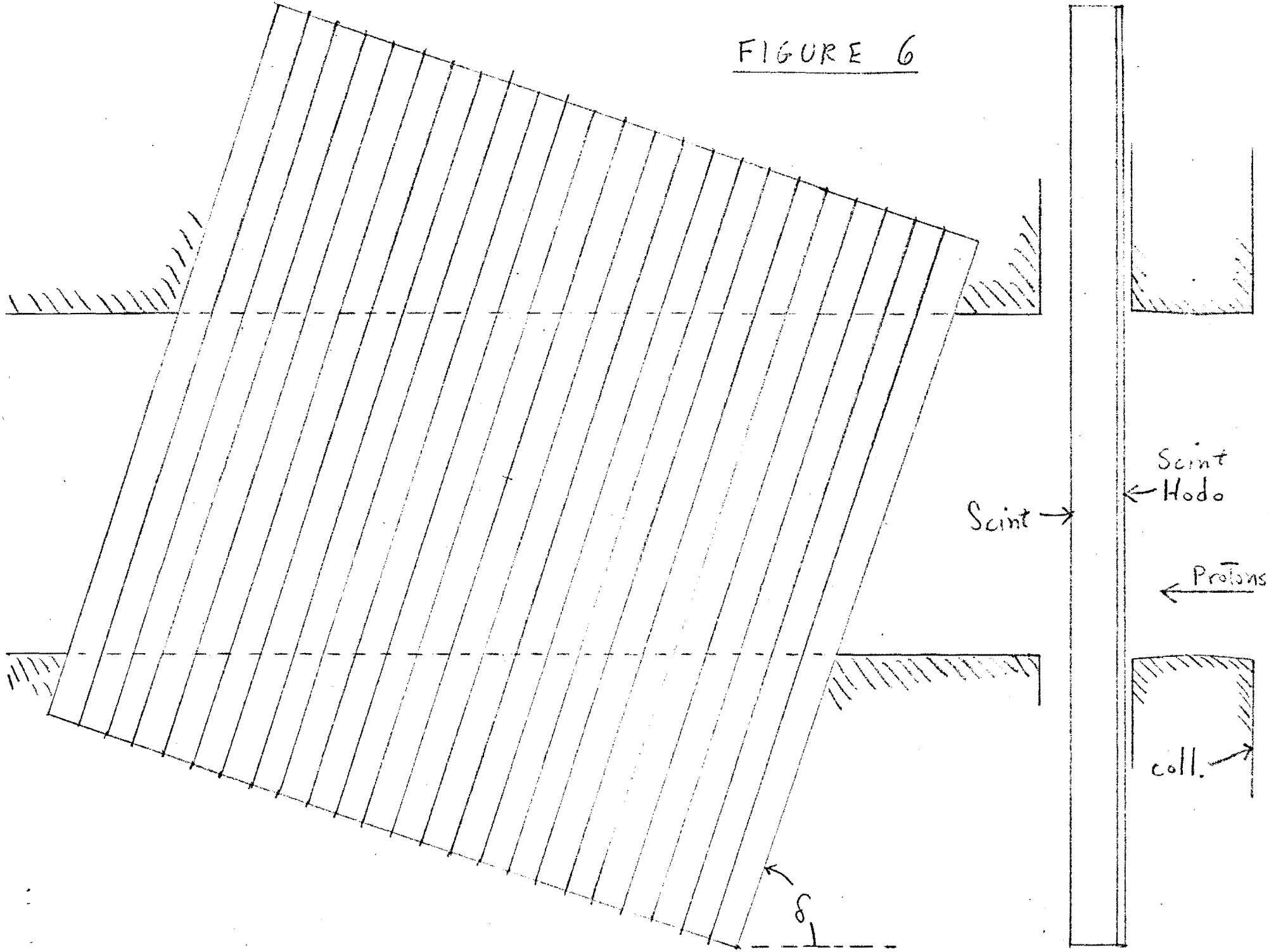

July 31, 1970

Addendum to

NAL PROPOSAL #16, pp ELASTIC AND INELASTIC SCATTERING

A. R. Clark, T. Elioff, A. C. Entis, R. C. Field, D. Keefe,
L. T. Kerth R. C. Sah, W. A. Wenzel, plus GSRA's

Additional information about the experimental apparatus was requested of us during the last week of the summer study.

I. Figure 1 shows the differentially pumped gas target. The scheme has been briefly examined by some LRL engineers who see nothing mysterious or tricky. At the minimum/possible (L. Teng, private communication) beam tube dimensions the new estimated flow rate of the order of 2000 micron liters per second implies a thermal load of the order of one watt, if a cryogenic (helium) pump is used. The cost of the overall system would therefore be dominated by the installation cost of the minimum cryogenic system available (probably $15–20 K).

It has been suggested to us that a somewhat less expensive installation would probably be possible with a titanium bulk sublimation system (made by Varian and others); maintenance also might be simpler. We note that the use of helium as an alternative target gas (suggested by us and others) would present particular problems in pumping. In this case a cryoabsorption pump would probably be best, although diffusion pumps could be used if the helium flow rate were suitably reduced.

B. Following an examination of the tunnel (the help of T. Collins is gratefully acknowledged) a more careful layout was made of the two types of magnetic spectrometer being considered by us. These are shown in Figures 2 and 3. The quadrupole doublet shown in Figure 2 is the one used in previously in the Bevatron gas target experiment. The spectrometer

magnet shown in Figure 3 does not exist, although it is expected that a suitable coil and yoke can be located to accommodate the carefully tailored pole tips.

For either spectrometer vertical and horizontal collimators to define azimuthal acceptance and target size, respectively, would be rigidly mounted to the spectrometer, as would the small steering magnet ($\approx 10^4$ gauss–in.) used to select the angular range of the recoil protons. The whole assembly could therefore be pretested as a unit before being coupled to the accelerator through a bellows. In the case of the doublet quadrupole spectrometer, the precise momentum width is established by the pulse height spectrum in the solid state counters. For the dipole spectrometer the geometrical resolution determines this quantity, and a simple scintillation counter hodoscope can be used. The two alternatives represent therefore different levels of sophistication of magnetic spectrometers vis–a–vis electronics.

We believe that either system is feasible. Although we can fit either into the main ring tunnel, it would obviously be nice to have more room.

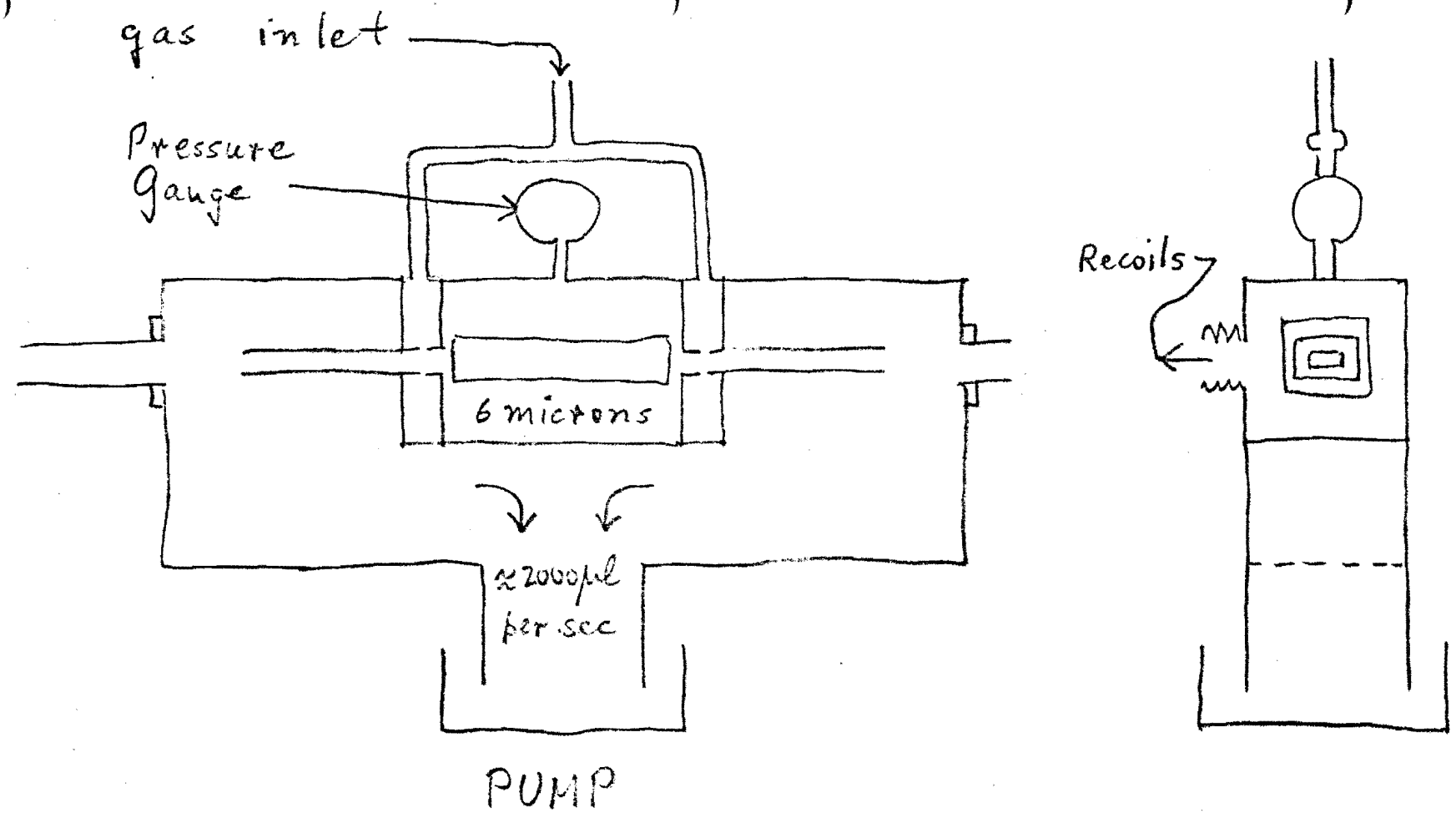

FIGURE 1

Addendum to NAL proposal #16

Addendum to NAL proposal #16

FIGURE 2

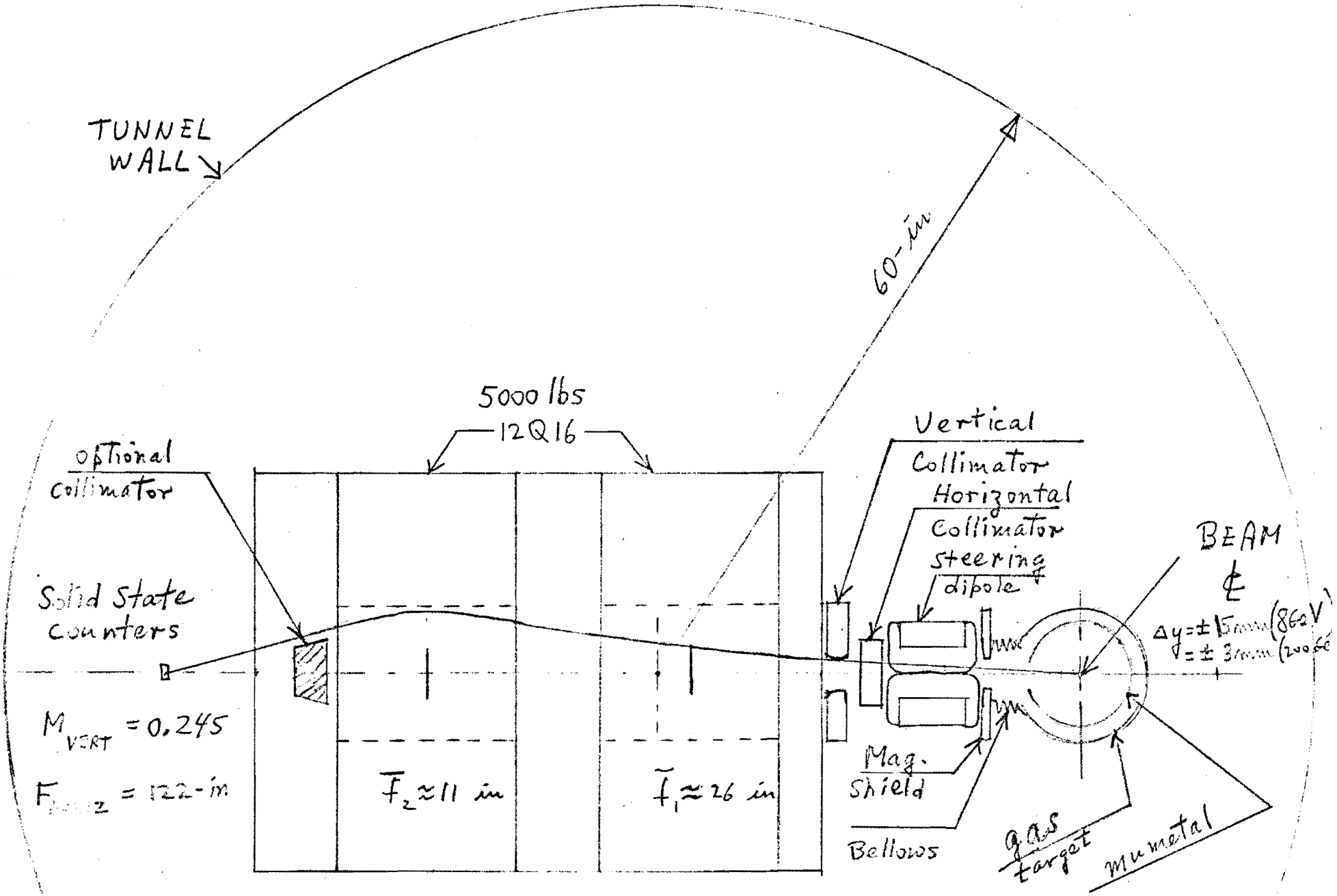

Addendum to NAL proposal #16

FIGURE 3